Generation of second harmonic radiation from sub-stoichiometric silicon nitride thin films

Emanuele Francesco Pecora, Antonio Capretti, Giovanni Miano, and Luca Dal Negro

Citation: Appl. Phys. Lett. **102**, 141114 (2013); doi: 10.1063/1.4801873
View online: http://dx.doi.org/10.1063/1.4801873
View Table of Contents: http://apl.aip.org/resource/1/APPLAB/v102/i14
Published by the American Institute of Physics.

Generation of second harmonic radiation from sub-stoichiometric silicon nitride thin films

Emanuele Francesco Pecora,[1] Antonio Capretti,[1,2] Giovanni Miano,[2] and Luca Dal Negro[1,3,a)]

[1]*Department of Electrical and Computer Engineering and Photonics Center, Boston University, 8 Saint Mary's Street, Boston, Massachusetts 02215, USA*

[2]*Department of Electrical Engineering and Information Technology, Università degli Studi di Napoli Federico II, Via Claudio 21, Napoli 80125, Italy*

[3]*Division of Materials Science & Engineering, Boston University, 15 Saint Mary's Street, Brookline, Massachusetts 02446, USA*

(Received 7 December 2012; accepted 1 April 2013; published online 12 April 2013)

Enhancing second-order optical processes in Si-compatible materials is important for the demonstration of innovative functionalities and nonlinear optical devices integrated on a chip. Here, we demonstrate significantly enhanced Second-Harmonic Generation (SHG) by silicon-rich silicon nitride materials over a broad spectral range, and show a maximum conversion efficiency of 4.5×10^{-6} for sub-stoichiometric samples with 46 at. % silicon. The SHG process in silicon nitride thin films is systematically investigated over a range of material stoichiometry and thermal annealing conditions. These findings can enable the engineering of innovative Si-based devices for nonlinear signal processing and sensing applications on a Si platform. © *2013 AIP Publishing LLC* [http://dx.doi.org/10.1063/1.4801873]

Nonlinear optical phenomena in silicon-based materials[1,2] have recently attracted significant attention due to the ability to control optical signals using light on a chip, thus potentially adding to the already successful silicon photonics platform innovative functionalities such as parametric down-conversion, multiple wavelength conversion, and all-optical signal routing for broadband signals processing.[3–8] However, Si is a centrosymmetric crystal and it exhibits a negligible second-order optical susceptibility $\chi^{(2)}$. The only sources of second-order nonlinearity arise from higher-order multipolar processes,[9] the breaking of crystal symmetry at the surface, or by the engineering of strain fields.[10–16] Despite recent advancements, the Second-Harmonic Generation (SHG) conversion efficiencies of Si-based materials remain low for nonlinear device applications and alternative materials need to be investigated. Here, we propose silicon-rich silicon nitride as a material for efficient SHG on Si. Silicon nitride already finds its place in the microelectronic industry as an insulator material and as a diffusion barrier, and its nonlinear generation efficiency is expected to be larger than in silicon due to reduced two-photon absorption.[17,18] Moreover, silicon-rich silicon nitride has been integrated with light emitting materials, waveguide structures, photonic crystal nano-cavities, plasmonic structures, and optical modulators.[19,20]

In this work, we systematically study the second-order nonlinear generation in Si-rich silicon nitride thin films of varying excess Si content and annealing conditions. In particular, we demonstrate visible SHG in the broad spectral range of 375 nm−450 nm, and we optimize the second harmonic emission at a silicon excess of 46 at. %, where we measured a maximum SHG efficiency of about 4.5×10^{-6}. Finally, we quantify the nonlinear behavior of the fabricated samples applying a model that describes the macroscopic nonlinear optical response of Si-rich nitride in terms of an effective second-order susceptibility.

Sub-stoichiometric silicon nitride thin films have been grown by N_2 reactive magnetron sputtering using Si target in a Denton Discovery 18 confocal-target sputtering system. The base pressure was about 4×10^{-7} mbar; the ratio between N_2 and Ar gas flow has been varied to control the Si content in the silicon nitride from the stoichiometric value (42.9%) up to 47.3%. Their thickness has been fixed at 200 nm. Samples have been grown at room temperature and post annealing processes were performed in a rapid thermal annealing furnace at temperatures between 500 °C and 900 °C for 200 s under forming gas atmosphere (5% H_2/95% N_2). The fabricated samples have been characterized by an Energy Dispersive X-Ray (EDX) Spectrometer (Oxford ISIS mounted in a Zeiss Supra 55 Scanning Electron Microscope) and their linear optical properties have been measured by optical transmission in a UV/VIS/NIR spectrophotometer (Varian/Agilent Cary 5000) and by spectroscopic ellipsometry (J. A. Woollam V-Vase). The nonlinear optical properties have been studied using a mode-locked high power ultrafast Ti:sapphire laser (MaiTai HP SpectraPhysics, 150 fs pulse width, 82 MHz repetition rate) with an average pumping power of 1 W, linearly polarized, and the excitation wavelength in the range of 750 nm−900 nm. For the polarization studies, the laser polarization has been varied using a half-wave liquid crystal variable retarder (Thorlabs LCC1111-B). The pump beam was focused on the sample using a 20× microscope objective. The angle of incidence was 45° and the reflected light has been collected through a standard telescoping lens arrangement. The pump light has been filtered before coupling the signal into an f/4 monochromator (Cornerstone 260). The SHG spectra have been detected

a)Author to whom correspondence should be addressed. Electronic mail: dalnegro@bu.edu.

with a lock-in amplifier (Oriel Merlin) coupled to a low light photomultiplier tube (PMT, Oriel Instrumentation 77348). A polarization analyzer was placed in front of the monochromator slits for polarization control. The SHG output power has been estimated considering the PMT responsivity, the measured transmittivity of all the optical components and the light coupling efficiency into the monochromator, and also directly measured through a highly sensitive power meter detector (Newport 918D-UV-OD3). The linear refractive indices of the fabricated samples have been measured and found in excellent agreement with the previously published data[21] on identically prepared samples as a function of the excess Si content measured using EDX.

In Fig. 1, we show the second harmonic spectra collected for the as-deposited sample with a silicon content of 46.2 at. % for different pumping wavelengths in the range between 750 nm and 900 nm. An identical trend has been observed also for all the other samples as a function of the pump wavelength. The SHG signal peaks at a pumping wavelength of 775 nm and the SHG power decreases when pumping at longer wavelengths.

In order to demonstrate the second-order nonlinear origin of the signals, we report in Fig. 2 the pump power dependence of the SHG output power at 375 nm. The best linear fit to the experimental data in log-log scale (continuous line) has a slope of 1.9 ± 0.1, consistently with the quadratic nature of the SHG process. Furthermore, in the inset of Fig. 2 we show the SHG peak wavelength as a function of the pump wavelength for the same sample, which exhibits a perfectly linear trend with slope 0.5, as expected for second-order nonlinear processes.

We have then studied the SHG intensity of Si-rich silicon nitride samples with a large range of fabrication parameters. Fig. 3 plots on a semi-logarithmic scale the SHG peak intensity measured for the as-deposited samples as a function of the Si content and for different excitation wavelengths, all excited at the same pump power. We can notice that all the samples exhibit a common trend, indicating that the Si excess plays a fundamental role in the second harmonic generation. The SHG intensity increases more than two orders of magnitude by increasing the excess Si in the samples, and

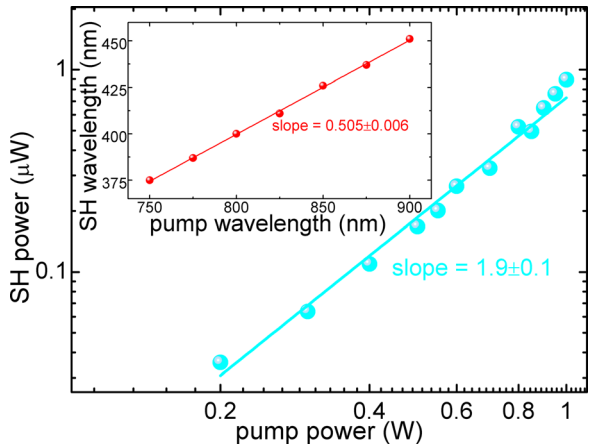

FIG. 2. Pump power dependence (log scale) of the emission peaked at 375 nm (750 nm excitation wavelength) from as-deposited silicon nitride with 46.2 at. % Si content. The continuous line is the best fit of the experimental data. (Inset) Measured second harmonic wavelength as a function of the excitation wavelength for the same sample. The continuous line is the linear fit of the experimental data.

best results are observed for samples with 46.2 at. % Si for all the wavelengths. A further increase in the Si excess reduces the SHG signal to values comparable with the ones measured for stoichiometric silicon nitride films.

We then performed rapid thermal annealing treatments at temperatures of 500 °C, 700 °C, and 900 °C on all the fabricated samples and report the SHG signal as a function of the annealing temperature for the sample with 46.2 at. % Si in Fig. 4. We note that the annealing treatment has a dramatic role in the SHG signal that decreases by almost two orders of magnitudes after annealing the samples. A similarly dramatic effect has been measured irrespective of the Si content in the samples, demonstrating that the as-deposited material is best suited for SHG. It is well-known that thermal annealing processes on silicon-rich silicon nitride and oxide materials are beneficial to saturate dangling bonds, create Si nanoclusters and enhance the light emission properties[21,22] as well as the energy transfer efficiency towards active rare earth dopants.[23–27] On the other hand, it has been recently demonstrated that as-deposited or low-temperature annealed silicon-rich silicon nitride and oxide films exhibit very large

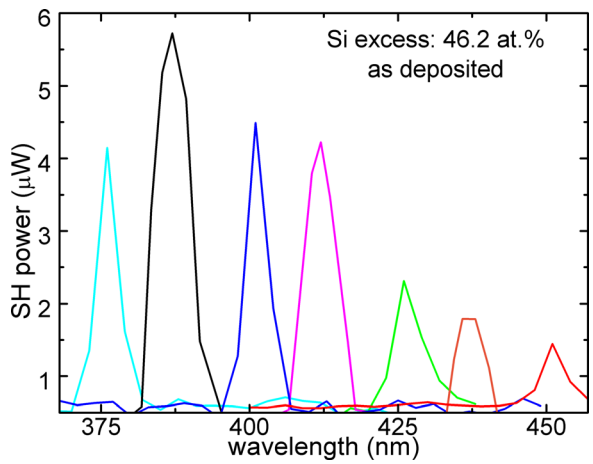

FIG. 1. Second harmonic spectra from as-deposited 46.2 at. % Si content silicon nitride after pumping with excitation wavelengths between 750 and 900 nm. All data have been taken at the same pumping power (1 W).

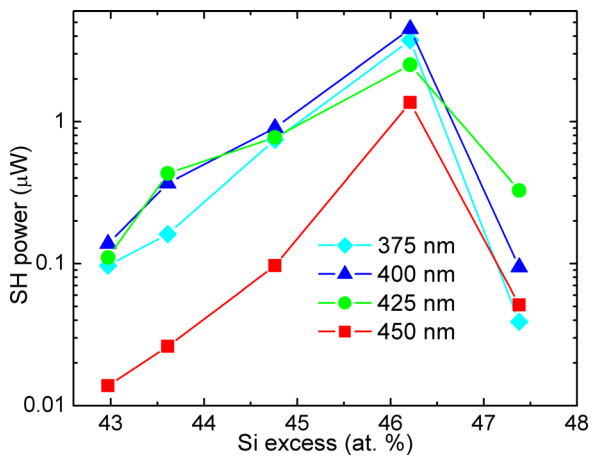

FIG. 3. Second harmonic power detected after pumping with different excitation wavelengths with the same pumping power as a function of the Si content.

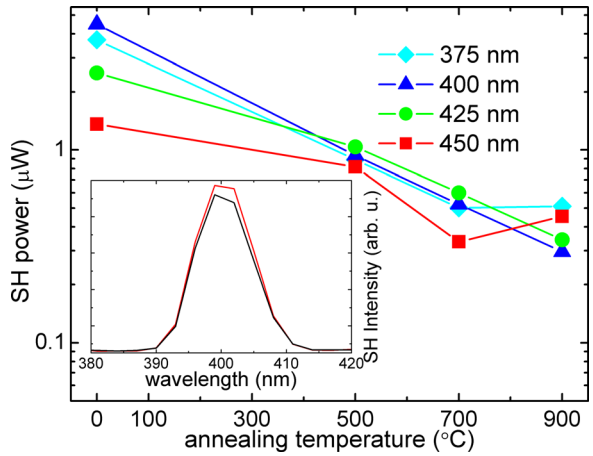

FIG. 4. Second harmonic power detected after pumping with different excitation wavelengths with the same pumping power as a function of the annealing temperature for the sample with 46.2 at. % Si content. (Inset) SH spectra for the as grown sample, with (black line) and without (red line) a 30 nm-thick SiO_2 cap layer.

nonlinear refractive index associated to the third-order susceptibility $\chi^{(3)}$.[28] In order to discriminate between the surface and the volume contributions to the observed SHG signal, we sputtered an optically thin (30 nm) SiO_2 layer atop the surface of the as-grown sample (46.2 at. % Si content), which is expected to quench the nonlinear surface dangling bonds that have been observed in similar samples.[29,30]

In the inset of Fig. 4, we show the SHG spectra measured for samples with and without the SiO_2 capping layer, and we notice that the SHG intensity is unchanged. This indicates that the observed second harmonic radiation is mostly generated from the bulk of the samples and that the contribution of the unpassivated Si nitride surface can be neglected.

In order to better understand the origin and the properties of the second harmonic signal, we performed polarization dependent SHG measurements and analyzed the s and p components (with respect to the reflection plane) of the nonlinear radiation as function of the polarization angle α of the pump beam. In Fig. 5, we show the polar plots of the SHG pumped at 800 nm in samples with different Si contents for the s (red dots) and p (blue circles) components. The top panel refers to the stoichiometric silicon nitride sample. While the p component is constant with respect to the pump polarization, the vertical component vanishes for $\alpha = 0°$, 90° (p- and s-polarized fundamental beams, respectively), and it exhibits its maximum intensity at around $\alpha = 45°$, 135°. This result is consistent with what already reported in the literature for the case of stoichiometric silicon nitride films,[18] owing to the in-plane isotropy (symmetry group $C_{\infty\nu}$) of SiN thin-films that deposited at low pressure (both by PECVD and sputtering) grow under significant conditions of compressive stress.[31,32] However, as the Si content is increased in the film, we observe a dramatic modification in the measured polar plots of the SHG. In particular, in the case of the most efficient sample with 46.2 at. % Si (bottom panel), the second harmonic has exactly the polarization of the pump, i.e., the s- (p-) component vanishes for $\alpha = 0°$ ($\alpha = 90°$), and it has maximum magnitude for $\alpha = 90°$ ($\alpha = 0°$). Therefore,

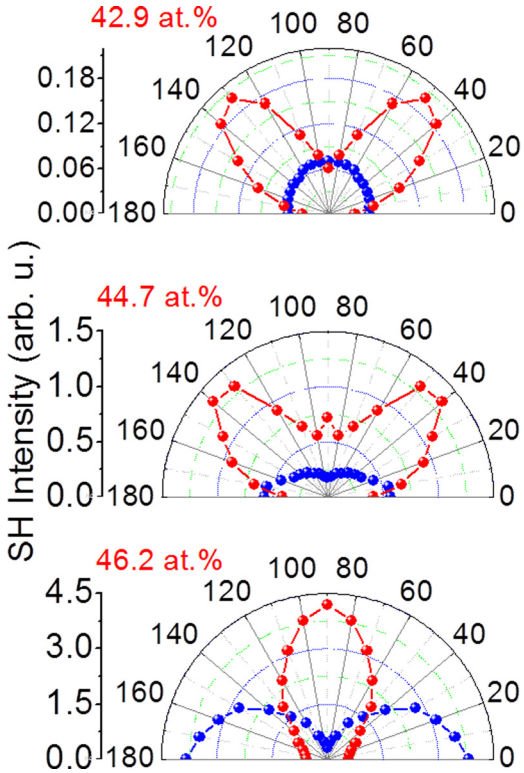

FIG. 5. Polar plots of the second harmonic intensity (arbitrary units) generated at a pumping wavelength of 800 nm in samples with different Si content, as-deposited. The pump polarization is changed and the detection polarization fixed at the s (red dots) and p (blue circles) polarization components. 0° corresponds to p-polarized pumping light; 90° to s-polarized pump.

the $C_{\infty\nu}$ symmetry is broken for Si-rich samples. We have already shown that the SHG intensity decreases by increasing the annealing temperature for all the investigated silicon nitride stoichiometry. For these reasons, our experimental data demonstrate that the strong nonlinear response measured for Si-rich films originates from either Si-related defects introduced by the excess Si in the matrix or from a high density of randomly distributed amorphous Si nanoclusters that nucleate within the non-stoichiometric SiN films.[33–36] The Si clustering in SiN thin films leads to the formation of small (<3 nm), almost spherical nanostructures across the sample. As a consequence, we effectively model their nonlinear response by considering randomly oriented dipole-like centers uniformly distributed in the sample. These data demonstrate that the introduction of excess Si in the Si nitride films with low temperature post-processing treatments has a very strong positive impact on the SHG properties.

In order to quantify the second-order nonlinear properties of sub-stoichiometric silicon nitride thin films, we measured the SHG efficiency for the as-deposited samples as a function of the Si content. The measured generation efficiencies are listed in Table I, along with the measured Tauc energy gaps and the refractive indices measured at 400 and at 800 nm. The measured SHG efficiency for the stoichiometric silicon nitride is 1.3×10^{-7} and this value increases by increasing the Si content up to 4.49×10^{-6} for a Si content of 46.2 at. %. Note that a further increase in the Si content is detrimental for the SHG efficiency, which drops to 9×10^{-8}, which is even lower than for stoichiometric silicon

TABLE I. Measured optical energy gap, linear refraction index at 400 and 800 nm, SHG efficiencies, and calculated $\chi^{(2)}$ tensorial elements for the different silicon contents in sub-stoichiometric silicon nitride thin films.

Si content (at. %)	Optical energy gap (eV)	SH efficiency	n at 400 nm	n at 800 nm	$\chi^{(2)}_{ttn}$ (pm/V)	$\chi^{(2)}_{ttt}$ (pm/V)
42.9	3.77	1.3×10^{-7}	2.07	1.89	14.82	…
43.6	3.52	3.6×10^{-7}	2.79	1.92	28.04	…
44.7	3.07	9.0×10^{-7}	3.38	2.02	37.89	28.56
46.2	2.50	4.49×10^{-6}	3.64	2.25	…	68.79
47.3	2.04	9×10^{-8}	4.40	2.35	…	10.08

nitride. We believe that at the highest Si concentrations dangling bonds and absorbing defects are formed in the matrix and increase the light absorption thus decreasing the overall SHG efficiency.

Finally, we apply the effective model described in Ref. 37 to quantify the second-order susceptibility $\chi^{(2)}$. According to this model, the field $\mathbf{E}_{int}^{(2\omega)}$ at the SHG frequency (2ω) inside the silicon nitride slab is expressed as the sum of the general solution of the associated homogeneous Helmholtz equation $\mathbf{E}_{int,hom}^{(2\omega)}$ and of the particular solution $\mathbf{E}_{int,par}^{(2\omega)}$. The field $\mathbf{E}_{ext}^{(2\omega)}$ radiated by the second harmonic sources is calculated by solving a characteristic system of linear equations. For the stoichiometric sample, the measured polarization diagram implies the $C_{\infty\nu}$ symmetry, and therefore the only non-vanishing components of $\chi^{(2)}$ are: $\chi_{ttn} = \chi_{tnt}$, χ_{ntt}, χ_{nnn}, where n indicates the normal to the film surface, and t indicates the tangent direction. The SHG p-component of the stoichiometric film is small with respect to the s-component. Therefore, we will consider only the s-component for the estimation of $\chi^{(2)}$ (only χ_{ttn} contributes to the SHG s-component). For Si-rich samples, the $C_{\infty\nu}$ symmetry is broken, and the experimental results in Fig. 5 indicate that χ_{ttt} is responsible for the SHG s-component. We estimate the tensorial elements χ_{ttn} and χ_{ttt} by fitting the experimental data with the presented model, with the assumption that the small Si clusters and the silicon nitride matrix contribute to the SHG radiation incoherently. At this wavelength, some absorption of the generated SH light may occur in the material due to the presence of Urbach tails.[35] As a consequence, part of the generated light does not escape from the sample and will not contribute to the measured efficiency. The results are shown in Table I, and in particular we predict $\chi_{ttt} = 68.79$ pm/V for the optimized sample.

In conclusion, we have demonstrated that Si-rich silicon nitride is a viable platform for efficient second harmonic generation in a Si-compatible material. We performed a systematic optimization of the SHG efficiency versus the material processing conditions and we measured a maximum generation efficiency of 4.49×10^{-6} for a Si content of 46% corresponding to an effective second-order susceptibility of about 70 pm/V. These findings can potentially enable innovative Si-based nonlinear optical devices for on-chip communications, sensing and optical processing applications.

This work was supported by the NSF Career Award No. ECCS-0846651, the AFOSR programs "Deterministic Aperiodic Structures for On-chip Nanophotonic and Nanoplasmonic Device Applications," under Award No. FA9550-10-1-0019, and the grant "Nanoscale Optical Emitters for High Density Information Processing using Photonic-Plasmonic Coupling in Coaxial Nanopillars" under Award No. FA9550-13-1-0011.

[1]R. L. Sutherland, *Handbook of Nonlinear Optics* (CRC Press, 2003).
[2]J. Leuthold, C. Koos, and W. Freude, Nature Photon. **4**, 535 (2010).
[3]M. A. Foster, A. C. Turner, J. E. Sharping, B. S. Schmidt, M. Lipson, and A. L. Gaeta, Nature **441**, 960 (2006).
[4]V. R. Almeida, C. A. Barrios, R. R. Panepucci, and M. Lipson, Nature **431**, 1081 (2004).
[5]A. M. Armani, R. P. Kulkarni, S. E. Fraser, R. C. Flagan, and K. J. Vahala, Science **317**, 783 (2007).
[6]J. T. Robinson, L. Chen, and M. Lipson, Opt. Express **16**, 4296 (2008).
[7]C. Koos, P. Vorreau, T. Vallaitis, P. Dumon, W. Bogaerts, R. Baets, B. Esembeson, I. Biaggio, T. Michinobu, and F. Diederich, Nature Photon. **3**, 216 (2009).
[8]R. Schnabel, N. Mavalvala, D. E. McClelland, and P. K. Lam, Nat. Commun. **1**, 121 (2010).
[9]D. Guidotti and T. A. Driscoll, Nuovo Cimento **8D**, 385 (1986).
[10]S. V. Govorkov, V. I. Emel'yanov, N. I. Koroteev, G. I. Petrov, I. L. Shumay, V. V. Yakovlev, and R. V. Khokhlov, J. Opt. Soc. Am. B **6**, 1117 (1989).
[11]J. Y. Huang, Jpn. J. Appl. Phys., Part 1 **33**, 3878 (1994).
[12]M. Falasconi, L. C. Andreani, A. M. Malvezzi, M. Patrini, V. Mulloni, and L. Pavesi, Surf. Sci. **481**, 105 (2001).
[13]J.-H. Zhao, Q. Chen, Z. Chen, G. Jia, W. Su, Y. Jiang, Z. Yan, T. V. Dolgova, O. A. Aktsipetrov, and H. Sun, Opt. Lett. **34**, 3340 (2009).
[14]C. Schriever, C. Bohley, and R. B. Wehrspohn, Opt. Lett. **35**, 273 (2010).
[15]S. A. Mitchell, M. Mehendale, D. M. Villeneuve, and R. Boukherroub, Surf. Sci. **448**, 367 (2001).
[16]M. Cazzanelli, F. Bianco, E. Borga, G. Pucker, M. Ghulinyan, E. Degoli, E. Luppi, V. Veniard, S. Ossicini, D. Modotto, S. Wabnitz, R. Pierobon, and L. Pavesi, Nature Mater. **11**, 148 (2012).
[17]J. S. Levy, M. A. Forster, A. L. Gaeta, and M. Lipson, Opt. Express **19**, 11415 (2011).
[18]T. Ning, H. Pietarinen, O. Hyvarinen, J. Simonen, G. Genty, and M. Kauranen, Appl. Phys. Lett. **100**, 161902 (2012).
[19]S. Yerci, R. Li, and L. Dal Negro, Appl. Phys. Lett. **97**, 081109 (2010).
[20]Y. Gong, M. Makarova, S. Yerci, R. Li, M. J. Stevens, B. Baek, S. W. Nam, R. H. Hadfield, S. N. Dorenbos, and V. Zwiller, Opt. Express **18**, 13863 (2010).
[21]S. Yerci, R. Li, O. Kucheyev, T. van Buuren, S. N. Basu, and L. Dal Negro, Appl. Phys. Lett. **95**, 031107 (2009).
[22]F. Iacona, C. Bongiorno, C. Spinella, S. Boninelli, and F. Priolo, J. Appl. Phys. **95**, 3723 (2004).
[23]G. Franzò, S. Boninelli, D. Pacifici, F. Priolo, F. Iacona, and C. Bongiorno, Appl. Phys. Lett. **82**, 3871 (2003).
[24]A. N. MacDonald, A. Hryciw, F. Lenz, and A. Meldrum, Appl. Phys. Lett. **89**, 173132 (2006).
[25]G. Franzò, E. F. Pecora, F. Priolo, and F. Iacona, Appl. Phys. Lett. **90**, 183102 (2007).
[26]R. Li, J. R. Schneck, J. Warga, L. D. Ziegler, and L. Dal Negro, Appl. Phys. Lett. **93**, 091119 (2008).
[27]E. F. Pecora, T. I. Murphy, and L. Dal Negro, Appl. Phys. Lett. **101**, 191115 (2012).
[28]S. Minissale, S. Yerci, and L. Dal Negro, Appl. Phys. Lett. **100**, 021109 (2012).
[29]W. M. M. Kessels, J. J. H. Gielis, I. M. Aarts, C. M. Leewis, and M. C. M. van de Sanden, Appl. Phys. Lett. **85**, 4049 (2004).
[30]S. Lettieri, F. Merola, P. Maddalena, C. Ricciardi, and F. Giorgis, Appl. Phys. Lett. **90**, 021919 (2007).

[31]S. Habermehl, J. Appl. Phys. **83**, 4672 (1998).
[32]J. H. Kim and K. W. Chung, J. Appl. Phys. **83**, 5831 (1998).
[33]V. M. Burlakov, G. A. D. Briggs, A. P. Sutton, A. Bongiorno, and A. Pasquarello, Phys. Rev. Lett. **93**, 135501 (2004).
[34]L. Dal Negro, R. Li, J. Warga, and S. N. Basu, Appl. Phys. Lett. **92**, 181105 (2008).
[35]S. Yerci, R. Li, S. O. Kucheyev, T. van Buuren, S. N. Basu, and L. Dal Negro, IEEE J. Quantum Electron. **16**, 114 (2010).
[36]G. Franzò, M. Miritello, S. Boninelli, R. Lo Savio, M. G. Grimaldi, F. Priolo, F. Iacona, G. Nicotra, C. Spinella, and S. Coffa, J. Appl. Phys. **104**, 094306 (2008).
[37]N. Bloembergen and P. S. Pershan, Phys. Rev. **128**, 606 (1962).